Supporting Information

Valant et al. 10.1073/pnas.1320962111

SI Materials and Methods

Materials. DMEM and hygromycin B were purchased from Invitrogen. FBS was purchased from ThermoTrace. [^{3}H]8-cyclopentyl-1,3-dipropylxanthine ([^{3}H]DPCPX; 120 Ci.mmol^{-1}), N^6-cyclohexyladenosine (5 Ci.mmol^{-1}), and [^{35}S]GTPγS (>1,000 Ci/mmol) were purchased from Perkin-Elmer. The Sure-Fire cellular ERK1/2 assay kits were a gift from TGR BioSciences. AlphaScreen reagents for ERK1/2 were from PerkinElmer Life Sciences. Ultima gold scintillation mixture was purchased from Packard Bioscience. VCP171 was synthesized in house as described previously (1). All orthosteric/allosteric hybrid ligands as well as the orthosteric with linker, VCP900, were synthesized in house. All other reagents were purchased from Sigma-Aldrich.

General Chemistry Experiment. A series of hybrid ligands, exhibiting both an orthosteric and an allosteric moiety, for the adenosine A_1 receptor (A_1AR) was designed and synthesized (Fig. 1 and Scheme S1). Melting points were determined with the Mettler Toledo MP50 melting point apparatus and are uncorrected. All reagents and anhydrous *N*,*N*-dimethylformamide (DMF) were purchased from Sigma-Aldrich and used without additional purification. Laboratory reagent-grade methanol, petroleum ether (40–60 °C), ethyl acetate, diethyl ether, and dichloromethane were purchased from Merck and used without additional purification. All ^{1}H NMR and ^{13}C NMR spectra were recorded on a Bruker Avance III 400 Ultrashield Plus spectrometer at 400.13 and 100.62 MHz, respectively. Unless stated otherwise, samples were dissolved in $CDCl_3$ Significant multiplicities are described by singlet (s), doublet (d), triplet (t), quadruplet (q), broad (br), multiplet (m), doublet of doublets (dd) or doublet of triplets (dt). Thin layer chromatography was conducted on 0.2-mm plates using Merck silica gel 60 F_{254}. Column chromatography was achieved using Merck silica gel 60 (particle size = 0.063–0.200 μm, 70–230 mesh), and eluent percentages are described in volume. High-resolution electrospray ionization (HR-ESI) mass spectra were obtained on a Waters LCT Premier XE (TOF). Compound purity was analyzed by liquid chromatography MS (LCMS; Agilent 1200 series LC coupled directly to a photodiode array detector and an Agilent 6100 Quadrupole MS) using a Phenomenex column (Luna 5-μm C8, 50 × 4.60 mm internal diameter). All compounds were >95% pure.

***N*-(3-benzoyl-5-iodo-4-(3-(trifluoromethyl)phenyl)thiophen-2-yl)acetamide (2).** A solution of **1** (8.56 g, 24.64 mmol) in acetic anhydride (20 mL) was refluxed for 5 min. The cooled mixture was concentrated to a residue that was taken up in ethyl acetate (200 mL) and washed with saturated bicarbonate solution (3 × 20 mL). The organic layer was dried ($MgSO_4$), filtered, and concentrated to a viscous resin that was taken up in acetic acid (90 mL), and *N*-iodosuccinimide (NIS) (6.10 g, 27.11 mmol) was added neat. The mixture was heated on an oil bath (45–50 °C) for several minutes, and then, a precipitate formed. The mixture was stirred for another 0.5 h at 45–50 °C. The mixture was cooled to room temperature, diluted while stirring with water (150 mL), and left to stir for another 10 min. The solid was filtered on a Buchner funnel/flask, washed with copious amounts of water, and suck-dried, providing **2** as a yellow solid (9.22 g, 73% yield). Mp 224–227 °C. ^{1}H NMR (400 MHz, DMSO) δ 11.13 (bs, 1H, NH), 7.50–7.41 (m, 3H, ArH), 7.41–7.29 (m, 4H, ArH), 7.28–7.17 (m, 2H, ArH), 2.15 (s, 3H, $COCH_3$). ^{13}C NMR (100 MHz, DMSO) δ 191.7, 168.6, 147.5, 140.7, 137.3, 137.1, 133.6, 132.7, 129.1, 129.0, 128.5 (q, J = 31.8 Hz), 128.0, 126.5–126.3 (m), 124.0–123.9 (m), 123.8 (q, J = 272.5 Hz), 122.7, 73.7, 22.4.

4-(5-Amino-4-benzoyl-3-(3-(trifluoromethyl)phenyl)thiophen-2-yl)benzoic acid (3). The iodide **2** (4.0 g, 7.76 mmol) was dissolved in DMF (50 mL), and 4-methoxycarbonylphenyl boronic acid (2.8 g, 15.53 mmol) was added followed by $Pd[PPh_3]_2Cl_2$ (0.54 g, 0.77 mmol) and 2 M K_3PO_4 (15 mL). The mixture was stirred and heated to 70 °C for 1 h under an N_2 atm. The cooled solution was slowly diluted with water (180 mL) while stirring, and a precipitate resulted. The heterogeneous mixture was stirred for another 15 min, and the solid was filtered on a Buchner funnel/flask, washed with copious amounts of water, and suck-dried. The solid was dissolved in a minimum of CH_2Cl_2 and filtered through a silica plug eluting with a 1:9 mixture of acetone to dichloromethane. The volatiles were removed under vacuum, resulting in a foam that was crystallized from 2-propanol, which provided the intermediate Suzuki product as a dark brown solid (3.63 g, 89% yield). ^{1}H NMR (400 MHz, DMSO) δ 11.04 (bs, 1H, NH), 7.86–7.72 (m, 2H, ArH), 7.55–7.47 (m, 2H, ArH), 7.44–7.36 (m, 2H, ArH), 7.29–7.17 (m, 7H, ArH), 3.80 (s, 3H, OCH_3), 2.16 (s, 3H, $COCH_3$). ^{13}C NMR (100 MHz, DMSO) δ 192.8, 168.5, 165.7, 142.6, 137.6, 137.6, 135.8, 134.0, 133.5, 132.8, 129.4, 129.1, 129.1, 129.0, 128.9, 128.8 (q, J = 31.7 Hz), 128.2, 128.0, 126.7–126.5 (m), 126.1 (q, J = 265.4 Hz), 124.4, 123.9–123.7 (m), 52.1, 22.6.

The intermediate Suzuki product (1.8 g, 3.44 mmol) was suspended in EtOH:H_2O (1:1). NaOH (1.4 g, 35.0 mmol) was added, and the reaction mixture was stirred on an oil bath (45–50 °C) for 3 h. The cooled solution was filtered through a Celite pad, and the filtrate was diluted with water (60 mL). The aqueous solution was chilled on an ice bath with stirring and carefully acidified to pH 2 with immediate precipitation of a yellow solid. The solid was filtered on a Buchner funnel/flask, washed with copious amounts of water, and suction-dried to yield **3** as a yellow powder (1.6 g, 99% yield). A small portion was recrystallized from 2-propanol. Mp 289–293 °C. ^{1}H NMR (400 MHz, DMSO) δ 12.93 (s, 1H, CO_2H), 8.31 (bs, 2H, NH_2), 7.77–7.66 (m, 2H, ArH), 7.25–7.20 (m, 1H, ArH), 7.19–6.97 (m, 8H, ArH), 6.99–6.87 (m, 1H, ArH). ^{13}C NMR (100 MHz, DMSO) δ 191.8, 166.9, 166.2, 140.2, 138.0, 136.8, 135.3, 134.2, 130.1, 129.9, 129.4, 128.7, 128.7, 128.5 (q, J = 32.8 Hz), 128.0, 127.2, 127.0 (q, J = 3.6 Hz), 123.8 (q, J = 272.4 Hz), 123.5–123.0 (m), 118.6, 115.5. LCMS R_f (min) = 6.13. MS m/z 468.0 (M + H). HR-ESIMS calculated for $C_{25}H_{17}F_3NO_3S^+$ (M + 1) 468.0876, found 468.0877.

General Procedure for the Synthesis of 5a–5f. The acid **3** (0.1 g, 0.214 mmol) was suspended in DMF (3 mL), and the amine (0.214 mmol) was added followed by (benzotriazol-1-yloxy)tris (dimethylamino)phosphonium hexafluorophosphate (BOP) reagent (0.142 g, 0.321 mmol) and finally, Et_3N (0.149 mL, 1.07 mmol). The mixture was left to stir at room temperature for 1–3 h. The mixture was slowly diluted with water (10 mL), and a resinous precipitate formed. The solvent was carefully decanted, and the precipitate was stirred in water (10 mL) for 0.5 h; the solvent carefully decanted. The crude product was chromatographed on silica gel, eluting with $CHCl_3$:MeOH:NH_4OH (90:10:1). The appropriate fractions were pooled and concentrated to a resin that was crystallized by trituration with a minimum amount of methanol. The solid was filtered on a Buchner funnel/flask and washed with a small amount of ice-cold methanol and finally, diethyl ether, providing **5a–5f** as yellow powders.

4-(5-Amino-4-benzoyl-3-(3-(trifluoromethyl)phenyl)thiophen-2-yl)-*N*-(2-(9-((2*R*,3*R*,4*S*,5*R*)-3,4-dihydroxy-5-(hydroxymethyl)tetrahydrofuran-2-yl)-9*H*-purin-6-ylamino)ethyl)benzamide (5a). Yield = 0.130 g, 80%. Mp 149–159 °C. ^{1}H NMR (400 MHz, DMSO) δ 8.58–8.44 (m, 1H),

8.37 (s, 1H), 8.30–8.15 (m, 3H), 8.07–7.92 (m, 1H), 7.65 (d, J = 8.4 Hz, 2H), 7.29–7.20 (m, 1H), 7.15–7.05 (m, 6H), 7.03–6.91 (m, 4H), 5.92 (d, J = 6.1 Hz, 1H), 5.47 (dd, J = 6.8, 4.2 Hz, 2H), 5.22 (d, J = 4.6 Hz, 1H), 4.64 (dd, J = 11.2, 6.0 Hz, 1H), 4.18 (dd, J = 8.1, 5.1 Hz, 1H), 4.00 (dd, J = 6.3, 3.2 Hz, 1H), 3.76–3.44 (m, 8H). ^{13}C NMR (100 MHz, DMSO) δ 191.9, 166.2, 165.9, 154.8, 152.4, 148.4, 140.3, 140.0, 136.9, 136.3, 134.9, 134.3, 132.5, 129.9, 128.8, 128.5 (q, J = 31.6 Hz), 128.4, 128.0, 127.4, 127.3, 127.1, 123.9 (q, J = 272.4 Hz), 123.3, 120.0, 118.9, 115.5, 88.1, 86.1, 73.6, 70.8, 61.8, 48.7. LCMS R_f (min) = 5.60. MS m/z 760.0 (M + H). HR-ESIMS calculated for $C_{37}H_{33}F_3N_7O_6S^+$ (M + 1) 760.2160, found 760.2176.

4-(5-Amino-4-benzoyl-3-(3-(trifluoromethyl)phenyl)thiophen-2-yl)-*N*-(4-(9-((2*R*,3*R*,4*S*,5*R*)-3,4-dihydroxy-5-(hydroxymethyl)tetrahydrofuran-2-yl)-9*H*-purin-6-ylamino)butyl)benzamide (5b). Yield = 0.060 g, 36% yield. Mp 130–143 °C. ^{1}H NMR (400 MHz, DMSO) δ 8.44–8.28 (m, 2H), 8.27–8.11 (m, 3H), 7.87 (s, 1H), 7.62 (d, J = 8.5 Hz, 2H), 7.29–7.18 (m, 1H), 7.17–7.05 (m, 6H), 7.05–6.84 (m, 4H), 5.88 (d, J = 6.2 Hz, 1H), 5.47–5.38 (m, 2H), 5.17 (d, J = 4.6 Hz, 1H), 4.61 (dd, J = 11.3, 6.1 Hz, 1H), 4.15 (dt, J = 7.8, 4.0 Hz, 1H), 3.97 (q, J = 3.4 Hz, 1H), 3.67 (dt, J = 12.0, 4.0 Hz, 1H), 3.62–3.37 (m, 3H), 3.23 (dd, J = 12.4, 6.5 Hz, 2H), 1.74–1.36 (m, 4H). ^{13}C NMR (100 MHz, DMSO) δ 191.7, 166.0, 165.4, 154.7, 152.4, 148.2, 140.2, 139.6, 136.9, 136.1, 134.8, 134.2, 132.6, 129.8, 128.7, 128.4, 128.3 (q, J = 31.6 Hz), 127.9, 127.2, 127.1, 127.0 (q, J = 3.4 Hz), 123.8 (q, J = 272.4 Hz), 123.2–123.1 (m), 119.7, 118.8, 115.4, 88.0, 85.9, 73.5, 70.7, 61.7, 39.0, 26.6. LCMS R_f (min) = 5.54. MS m/z 788.0 (M + H). HR-ESIMS calculated for $C_{39}H_{37}F_3N_7O_6S^+$ (M + 1) 788.2473, found 788.2495.

4-(5-Amino-4-benzoyl-3-(3-(trifluoromethyl)phenyl)thiophen-2-yl)-*N*-(6-(9-((2*R*,3*R*,4*S*,5*R*)-3,4-dihydroxy-5-(hydroxymethyl)tetrahydrofuran-2-yl)-9*H*-purin-6-ylamino)hexyl)benzamide (5c; VCP746). Yield = 0.092 g, 53% yield. Mp 126–138 °C. ^{1}H NMR (400 MHz, DMSO) δ 8.38–8.27 (m, 2H), 8.27–8.05 (m, 3H), 7.86 (s, 1H), 7.63 (d, J = 8.5 Hz, 2H), 7.29–7.19 (m, 1H), 7.19–7.04 (m, 6H), 7.04–6.84 (m, 4H), 5.89 (d, J = 6.2 Hz, 1H), 5.53–5.34 (m, 2H), 5.18 (d, J = 4.6 Hz, 1H), 4.62 (dd, J = 11.3, 6.1 Hz, 1H), 4.16 (dd, J = 7.7, 4.7 Hz, 1H), 3.98 (q, J = 3.3 Hz, 1H), 3.68 (dt, J = 12.0, 4.0 Hz, 1H), 3.62–3.37 (m, 3H), 3.19 (dd, J = 12.7, 6.5 Hz, 2H), 1.67–1.17 (m, 8H). ^{13}C NMR (100 MHz, DMSO) δ 191.8, 166.0, 165.4, 154.7, 152.4, 148.2, 140.2, 139.6, 136.9, 136.1, 134.8, 134.3, 132.7, 129.8, 128.7, 128.4, 128.3 (q, J = 31.6 Hz), 127.9, 127.2, 127.2–126.9 (m), 127.1, 123.8 (q, J = 272.4 Hz), 123.2 (q, J = 4.0 Hz), 119.7, 118.8, 115.4, 88.0, 86.0, 73.5, 70.7, 61.7, 39.2, 29.1, 26.3, 26.2. LCMS R_f (min) = 5.66. MS m/z 816.2 (M + H). HR-ESIMS calculated for $C_{41}H_{41}F_3N_7O_6S^+$ (M + 1) 816.2786, found 816.2800.

4-(5-Amino-4-benzoyl-3-(3-(trifluoromethyl)phenyl)thiophen-2-yl)-*N*-(8-(9-((2*R*,3*R*,4*S*,5*R*)-3,4-dihydroxy-5-(hydroxymethyl)tetrahydrofuran-2-yl)-9*H*-purin-6-ylamino)octyl)benzamide (5d). Yield = 0.102 g, 57% yield. Mp 122–132 °C. ^{1}H NMR (400 MHz, DMSO) δ 8.47–8.27 (m, 2H), 8.27–7.97 (m, 3H), 7.85 (s, 1H), 7.64 (d, J = 8.5 Hz, 2H), 7.30–7.20 (m, 1H), 7.19–7.05 (m, 6H), 7.04–6.74 (m, 4H), 5.90 (d, J = 6.2 Hz, 1H), 5.60–5.29 (m, 2H), 5.18 (d, J = 4.6 Hz, 1H), 4.63 (dd, J = 11.3, 6.1 Hz, 1H), 4.17 (dd, J = 7.7, 4.7 Hz, 1H), 3.99 (q, J = 3.2 Hz, 1H), 3.69 (dt, J = 11.9, 3.9 Hz, 1H), 3.63–3.40 (m, 3H), 3.25–3.10 (m, 2H), 1.78–1.13 (m, 12H). ^{13}C NMR (100 MHz, DMSO) δ 191.8, 166.0, 165.4, 154.7, 152.4, 148.2, 140.2, 139.6, 136.9, 136.1, 134.8, 134.3, 132.7, 129.8, 128.7, 128.4, 128.4 (q, J = 31.6 Hz), 127.9, 127.2, 127.2, 127.1–126.9 (m), 123.8 (q, J = 272.5 Hz), 123.2 (q, J = 3.2 Hz), 119.8, 118.8, 115.4, 88.1, 86.0, 73.5, 70.7, 61.7, 48.6, 39.2, 29.1, 2 × 28.8, 26.5, 26.4. LCMS R_f (min) = 5.86. MS m/z 844.1 (M + H). HR-ESIMS calculated for $C_{43}H_{45}F_3N_7O_6S^+$ (M + 1) 844.3099, found 844.3121.

4-(5-Amino-4-benzoyl-3-(3-(trifluoromethyl)phenyl)thiophen-2-yl)-*N*-(10-(9-((2*R*,3*R*,4*S*,5*R*)-3,4-dihydroxy-5-(hydroxymethyl)tetrahydrofuran-2-yl)-9*H*-purin-6-ylamino)decyl)benzamide (5e). Yield = 0.07 g, 37% yield. Mp 122–131 °C. ^{1}H NMR (400 MHz, DMSO) δ 8.38–8.27 (m, 2H), 8.28–7.99 (m, 3H), 7.85 (s, 1H), 7.63 (d, J = 8.5 Hz, 2H), 7.30–7.18 (m, 1H), 7.18–7.05 (m, 6H), 7.05–6.85 (m, 4H), 5.89 (d, J = 6.2 Hz, 1H), 5.54–5.32 (m, 2H), 5.18 (d, J = 4.6 Hz, 1H), 4.62 (dd, J = 11.3, 6.1 Hz, 1H), 4.16 (dd, J = 7.7, 4.7 Hz, 1H), 3.98 (q, J = 3.3 Hz, 1H), 3.68 (dt, J = 12.0, 4.0 Hz, 1H), 3.62–3.36 (m, 3H), 3.18 (dd, J = 12.8, 6.6 Hz, 2H), 1.67–1.37 (m, 4H), 1.37–1.12 (m, 12H). ^{13}C NMR (100 MHz, DMSO) δ 191.7, 166.0, 165.3, 154.7, 152.3, 148.2, 140.1, 139.6, 136.8, 136.0, 134.7, 134.2, 132.6, 129.8, 128.6, 128.4, 128.3 (q, J = 31.6 Hz), 127.9, 127.2, 127.1, 127.0 (q, J = 3.4 Hz), 123.7 (q, J = 272.4 Hz), 123.1 (q, J = 3.4 Hz), 119.7, 118.7, 88.0, 85.9, 73.5, 70.7, 61.7, 39.1, 29.0, 28.9, 28.9, 28.8, 28.7, 26.4, 26.4. LCMS R_f (min) = 6.05. MS m/z 872.1 (M + H). HR-ESIMS calculated for $C_{45}H_{49}F_3N_7O_6S^+$ (M + 1) 872.3412, found 872.3428.

4-(5-Amino-4-benzoyl-3-(3-(trifluoromethyl)phenyl)thiophen-2-yl)-*N*-(12-(9-((2*R*,3*R*,4*S*,5*R*)-3,4-dihydroxy-5-(hydroxymethyl)tetrahydrofuran-2-yl)-9*H*-purin-6-ylamino)dodecyl)benzamide (5f). Yield = 0.109 g, 57%. Mp 114–125 °C. ^{1}H NMR (400 MHz, DMSO) δ 8.41–8.28 (m, 2H), 8.28–8.06 (m, 3H), 7.84 (s, 1H), 7.64 (d, J = 8.4 Hz, 2H), 7.30–7.19 (m, 1H), 7.19–7.05 (m, 6H), 7.04–6.80 (m, 4H), 5.91 (d, J = 6.1 Hz, 1H), 5.60–5.32 (m, 2H), 5.19 (d, J = 4.6 Hz, 1H), 4.64 (dd, J = 11.3, 6.0 Hz, 1H), 4.18 (dd, J = 7.6, 4.6 Hz, 1H), 4.08–3.89 (m, 1H), 3.70 (dt, J = 11.8, 3.8 Hz, 1H), 3.64–3.40 (m, 3H), 3.19 (dd, J = 12.4, 6.5 Hz, 2H), 1.72–1.07 (m, 20H). ^{13}C NMR (100 MHz, DMSO) δ 191.8, 166.1, 165.4, 154.7, 152.4, 148.2, 140.2, 139.6, 136.9, 136.1, 134.8, 134.2, 132.7, 129.8, 128.7, 128.4, 128.4 (q, J = 31.7 Hz), 127.9, 127.3, 127.2, 127.0 (q, J = 3.4 Hz), 123.8 (q, J = 272.4 Hz), 123.2–123.1 (m), 119.8, 118.8, 115.5, 88.1, 86.0, 73.6, 70.8, 61.8, 39.2, 2 × 29.1, 3 × 29.0, 28.9, 28.8, 26.5, 26.5. LCMS R_f (min) = 6.34. MS m/z 900.0 (M + H). HR-ESIMS calculated for $C_{47}H_{53}F_3N_7O_6S^+$ (M + 1) 900.3725, found 900.3738.

***N*-(6-((9-((2*R*,3*R*,4*S*,5*R*)-3,4-dihydroxy-5-(hydroxymethyl)tetrahydrofuran-2-yl)-9*H*-purin-6-yl)amino)hexyl)benzamide (6; VCP900).** Benzoic acid (0.05 g, 0.409 mmol) was dissolved in DMF (2 mL), and the amine **4** (0.1 g, 0.273 mmol) was added followed by BOP reagent (0.241 g, 0.546 mmol) and finally, *N*,*N*-diispropylethylamine (DIPEA) (0.190 mL, 1.092 mmol). The mixture was left to stir at room temperature overnight. The mixture was slowly diluted with water (10 mL) and extracted with EtOAc (2 × 50 mL). The combined organic layers were washed with water (2 × 20 mL) and finally, brine (20 mL), dried ($MgSO_4$), filtered, and concentrated to a residue. The residue was chromatographed on silica gel, eluting with $CHCl_3$:MeOH:NH_4OH (90:10:1) to yield the desired product as an amorphous white solid (0.043 g, 33% yield). ^{1}H NMR (400 MHz, DMSO) δ 8.43 (t, J = 5.4 Hz, 1H), 8.34 (s, 1H), 8.20 (bs, 1H), 7.97–7.85 (m, 1H), 7.85–7.80 (m, 2H), 7.52–7.41 (m, 3H), 5.90 (d, J = 6.2 Hz, 1H), 5.53–5.40 (m, 2H), 5.20 (d, J = 4.6 Hz, 1H), 4.63 (dd, J = 11.2, 6.0 Hz, 1H), 4.16 (dd, J = 7.6, 4.6 Hz, 1H), 4.01–3.93 (m, 1H), 3.73–3.65 (m, 1H), 3.60–3.53 (m, 1H), 3.52–3.40 (m, 2H), 3.25 (dd, J = 12.8, 6.6 Hz, 2H), 1.69–1.48 (m, 4H), 1.44–1.25 (m, 4H). ^{13}C NMR (101 MHz, DMSO) δ 166.1, 154.7, 152.4, 148.2, 139.7, 134.8, 131.0, 128.2, 127.1, 119.8, 88.1, 86.0, 73.5, 70.7, 64.9, 61.8, 39.2, 29.2, 29.1, 26.4, 26.2. LCMS R_f (min) = 5.02. MS m/z 471.3 (M + H). HR-ESIMS calculated for $C_{23}H_{31}N_6O_5^+$ (M + 1) 471.2350, found 471.2354.

Cell Culture and Membrane Preparation. FlpIn-CHO cells stably expressing the A_1AR were generated and cultured as described previously (2). Membranes of A_1ARs were generated as described previously (2). H9c2(2-1) rat cardiomyoblast cells were cultured as described previously (3, 4). Neonatal cardiomyocytes were isolated and cultured as described previously (5). All experiments were performed under approval from the Monash University Animal Ethics Committee.

Radioligand Equilibrium Binding Assays. For whole-cell binding, FlpIn-CHO cells stably expressing the A_1AR were seeded at a density of 3×10^4 cells/well into 96-well culture plates and incubated overnight at 37 °C in 5% CO_2. Growth media were replaced with binding buffer (DMEM containing 25 mM Hepes) containing 1 nM [^{3}H]DPCPX (K_I = 1.2 nM) and increasing concentrations of unlabeled ligand. Cells were incubated 60 min at 30 °C; then, media were removed followed by two washes in ice-cold 0.9% NaCl buffer to remove unbound radioligand. Cells were solubilized in 0.1 M NaOH, samples were transferred into a tube containing 4 mL scintillant (IRGA-Safe plus; PerkinElmer Life Sciences), and radioactivity was determined by β-counting. Non-specific binding was defined by 100 μM R-PIA.

Cell Signaling Assays. Studies of ERK1/2 phosphorylation (pERK1/2), inhibition of cAMP accumulation, and [^{35}S]GTPγS binding assays were performed as described previously (6, 7). For pERK1/2 experiments, 10% (vol/vol) FBS was used as a positive control, and vehicle controls were also performed; for both functional assays, pERK1/2 and [^{35}S]GTPγS binding assays data were normalized to the maximal response elicited by 10 μM adenosine or R-PIA (as specified).

Data Analysis. Computerized nonlinear regression was performed using Prism 6.0 (GraphPad Software). Radioligand inhibition binding data with competitive ligands were empirically fitted to a one-site inhibition mass action curve to determine inhibitor potency estimates, which were then converted to K_I values as appropriate (8), whereas the inhibition binding curve of VPC171 was fitted to a simple allosteric ternary complex model to derive estimates of allosteric modulator affinity (K_B) and cooperativity (α), the latter parameter being a measure of the strength and direction of the interaction between the orthosteric and allosteric sites (9); values of $\alpha > 1$ denote positive cooperativity, whereas values of $0 < \alpha < 1$ denote negative cooperativity. Where appropriate, concentration–response curves were fitted to a three-parameter logistic equation to derive the ligand potency estimate (pEC_{50}) and the maximal agonist effect (E_{max}). Finally, for whole-cell functional ligand combination studies, the interaction between the orthosteric agonist, R-PIA, and the competitive antagonist ligand, DPCPX, was fitted to a Waud/Schild model of competitive interaction (built into GraphPad Prism), whereas the interaction between VCP746 and DPCPX was not fitted to a specific model because of the mixed mode of orthosteric/allosteric behavior; instead, the concentration–response data were empirically fitted to a logistic equation.

To quantify signaling bias, agonist concentration–response curves were analyzed by nonlinear regression using an operational model of agonism (10) to define τ/K_A ratios for each agonist for each pathway according to the following equation:

$$Y = \text{basal} + \frac{(E_m - \text{basal}) \times \left(\frac{\tau}{K_A}\right)^n \times [A]^n}{[A]^n \times \left(\frac{\tau}{K_A}\right)^n + \left(1 + \frac{[A]}{K_A}\right)^n},$$

where E_m is the maximal possible response of the system (not the agonist), basal is the basal level of response in the absence of agonist, K_A denotes the functional equilibrium dissociation constant of the agonist for the receptor, n is the slope of the transducer function that links occupancy to response, and τ/K_A (transduction ratio estimated as a single fitted parameter) incorporates the affinity of the agonist for the active state of the receptor that triggers signaling (K_A) as well as the efficiency of coupling of the receptor to its subsequent cellular stimulus–response transduction mechanisms (τ). The estimated τ/K_A values were then used in the comparison of biased agonism mediated by each agonist across the various pathways (10). To exclude possible bias introduced by the cellular host system, the transduction ratios derived from application of the operational model of agonism were normalized to the transduction ratio of a reference agonist (in this case, the chemically stable agonist R-PIA). Under these conditions, if the test agonist and the reference agonist activate the two pathways through a common receptor conformation, the log[bias factor] should be 0.0 (or bias factor different from 1.0), irrespective of differences in response amplification between pathways. In contrast, significant deviation of log[bias factor] from 0.0 (or bias factor different from 1.0) indicates the involvement of distinct conformations for the different agonists.

1. Aurelio L, et al. (2009) Allosteric modulators of the adenosine A_1 receptor: Synthesis and pharmacological evaluation of 4-substituted 2-amino-3-benzoylthiophenes. *J Med Chem* 52 (14):4543–4547.
2. Stewart GD, et al. (2009) Determination of adenosine A_1 receptor agonist and antagonist pharmacology using Saccharomyces cerevisiae: Implications for ligand screening and functional selectivity. *J Pharmacol Exp Ther* 331(1):277–286.
3. Urmaliya VB, et al. (2010) A novel highly selective adenosine A_1 receptor agonist VCP28 reduces ischemia injury in a cardiac cell line and ischemia-reperfusion injury in isolated rat hearts at concentrations that do not affect heart rate. *J Cardiovasc Pharmacol* 56(3):282–292.
4. Urmaliya VB, et al. (2009) Cardioprotection induced by adenosine A_1 receptor agonists in a cardiac cell ischemia model involves cooperative activation of adenosine A_{2A} and A_{2B} receptors by endogenous adenosine. *J Cardiovasc Pharmacol* 53(5):424–433.
5. Lekawanvijit S, et al. (2010) Does indoxyl sulfate, a uraemic toxin, have direct effects on cardiac fibroblasts and myocytes? *Eur Heart J* 31(14):1771–1779.
6. Aurelio L, et al. (2009) Allosteric modulators of the adenosine A_1 receptor: Synthesis and pharmacological evaluation of 4-substituted 2-amino-3-benzoylthiophenes. *J Med Chem* 52 (14):4543–4547.
7. Valant C, et al. (2010) Delineating the mode of action of adenosine A_1 receptor allosteric modulators. *Mol Pharmacol* 78(3):444–455.
8. Cheng Y, Prusoff WH (1973) Relationship between the inhibition constant (K1) and the concentration of inhibitor which causes 50 per cent inhibition (I50) of an enzymatic reaction. *Biochem Pharmacol* 22(23):3099–3108.
9. Christopoulos A, Kenakin T (2002) G protein-coupled receptor allosterism and complexing. *Pharmacol Rev* 54(2):323–374.
10. Kenakin T, Watson C, Muniz-Medina V, Christopoulos A, Novick S (2012) A simple method for quantifying functional selectivity and agonist bias. *ACS Chem Neurosci* 3(3):193–203.

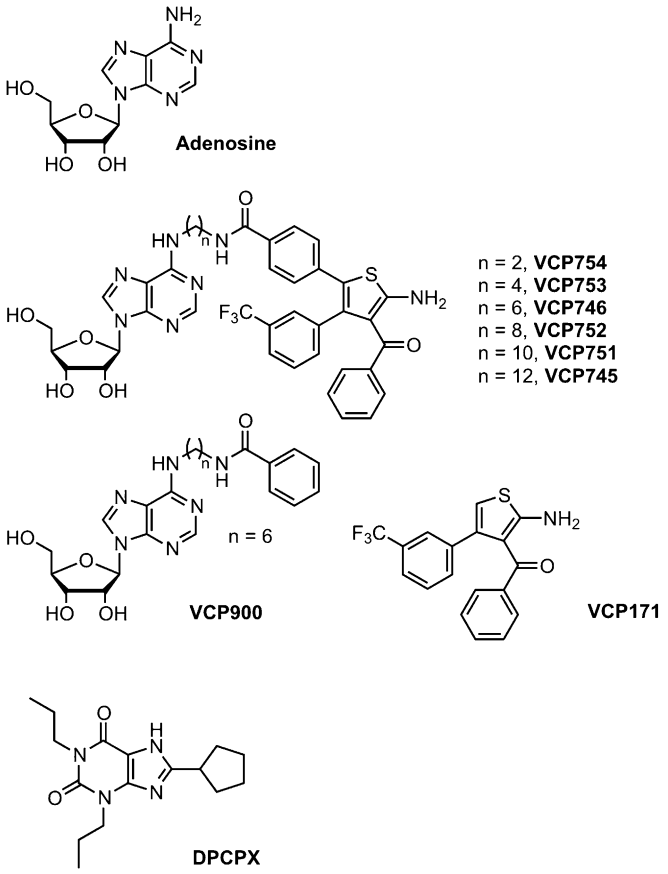

Fig. S1. Structures of hybrid and comparator ligands used in this study.

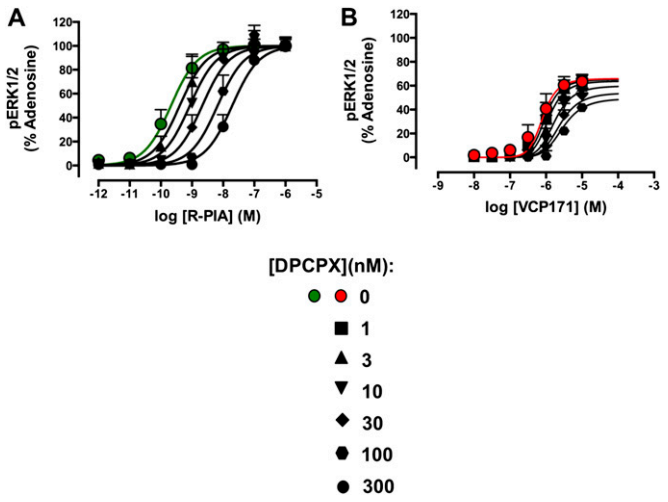

Fig. S2. Observed interaction between (*A*) R-PIA and DPCPX and (*B*) VCP171 and DPCPX in assays of A_1AR-mediated pERK1/2. Data represent the means of three experiments ± SEMs performed in duplicate.

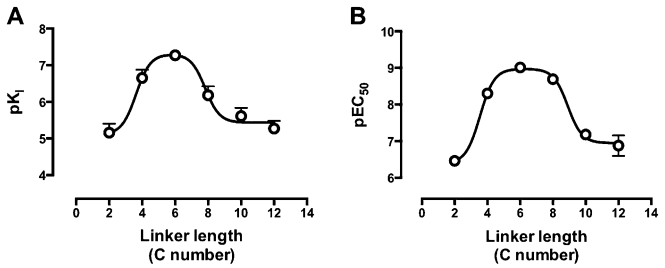

Fig. S3. The bell-shaped relationship observed between linker length and hybrid compound affinity and potency. (*A*) The affinity (pK_I) of hybrid compounds, determined in whole-cell radioligand binding assays, is plotted as a function of the carbon number within the linker region. (*B*) The potency (pEC_{50}) of hybrid compounds, determined in membrane-based [^{35}S]GTPγS binding assays, is plotted as a function of the carbon number within the linker region.

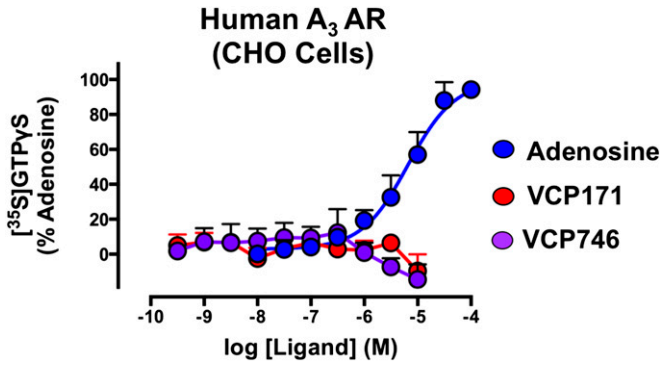

Fig. S4. VCP746 does not activate the adenosine A_3 receptor (A_3AR). Pharmacological characterization of the indicated ligands in membrane-based functional assays of [^{35}S]GTPγS binding in CHO cells stably expressing the human A_3AR. Data represent the means of three experiments ± SEMs performed in duplicate.

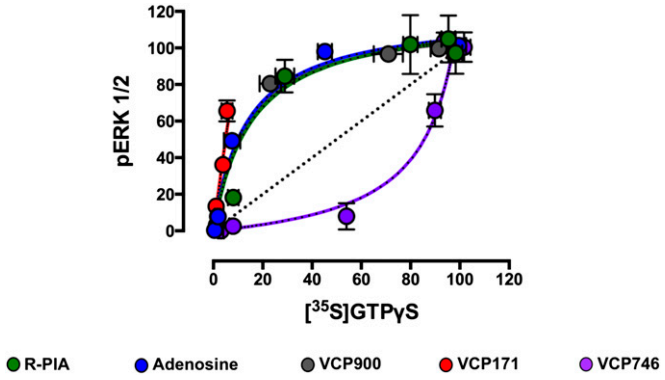

Fig. S5. Bias plots showing the effects to equimolar concentrations of each agonist at the [^{35}S]GTPγS vs. pERK1/2 pathways.

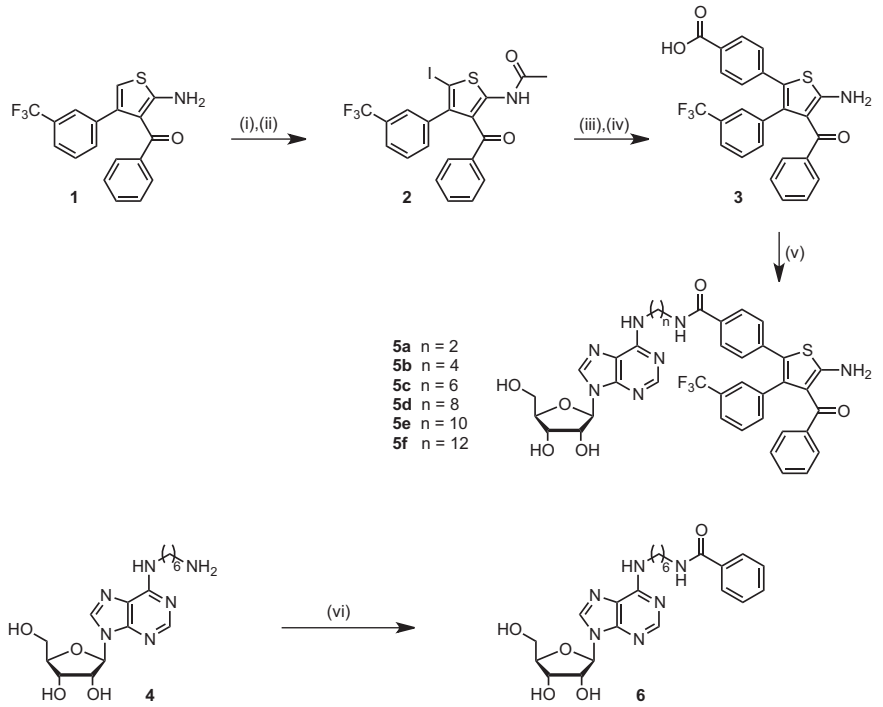

Scheme S1. (i) Ac_2O, reflux; (ii) AcOH, NIS; (iii) 4-$MeO_2CPhB(OH)_2$, Pd[PPh_3]$_2Cl_2$, 2 M K_3PO_4, DMF; (iv) NaOH, EtOH, H_2O; (v) **4**, BOP, NEt_3, DMF; (vi) $PhCO_2H$, BOP, DIPEA, DMF.

Table S1. Transduction coefficients [$\log_{10}(\tau/K_A)$], normalized transduction coefficients [$\Delta\log_{10}(\tau/K_A)$], and bias factors [$\Delta\Delta\log_{10}(\tau/K_A)$] for signaling at the A_1AR

	R-PIA	*N*6-cyclopentyladenosine (CPA)	Adenosine	VCP900	VCP746	VCP171
Log(τ/K_A)						
$[cAMP]_i$	8.96 ± 0.12	8.98 ± 0.10	7.62 ± 0.12	7.13 ± 0.14	9.21 ± 0.12	5.77 ± 0.41
pERK1/2	9.50 ± 0.09	9.59 ± 0.12	7.98 ± 0.09	7.35 ± 0.09	8.20 ± 0.09	6.04 ± 0.14
ΔLog(τ/K_A)						
$[cAMP]_i$	0 ± 0.17	0.02 ± 0.16	−1.34 ± 0.17	−1.83 ± 0.18	0.24 ± 0.17	−3.19 ± 0.42
pERK½	0 ± 0.13	0.09 ± 0.15	−1.52 ± 0.13	−2.14 ± 0.13	−1.29 ± 0.13	−3.46 ± 0.17
Log[bias factor]						
$[cAMP]_i$:pERK½*	0.00 ± 0.21 (1.0)	−0.07 ± 0.22	0.18 ± 0.21 (1.5)	0.31 ± 0.22 (2.0)	1.53 ± 0.21† (33.9)	0.27 ± 0.46 (1.9)

Data are means ± SEMs of three individual experiments performed in duplicate.
*Antilogarithm of the bias factor is shown in parentheses.
†Value statistically significant compared with R-PIA in one-way ANOVA followed by Dunnett's posttest.